(Received 17 October 2024, Accepted 3 December 2024, Scheduled 15 December 2024)

A Slot Array Cavity Backed SIW Metamaterial Antenna for Satellite Applications

Astha Sharma* and Reema Budhiraja

Jaypee Institute of Information Technology, Noida, India

ABSTRACT: This research paper presents a novel dual-band slot array cavity-backed metamaterial antenna designed using advanced substrate integrated waveguide (SIW) technology. The antenna is specifically optimized for operation in the Ka-band frequencies. The incorporation of slots in the proposed design yields substantial advantages, such as enhanced impedance matching, exceptional directivity, and the capability for dual-band operation. Furthermore, the designed antenna showcases a gain of 6.40 dBi at 27.42 GHz and 4.77 dBi at 28.70 GHz, which is a result of the innovative incorporation of metamaterials within the SIW cavity. This demonstrates the antenna's ability to provide efficient signal reception and transmission, particularly in the specified frequency bands. The antenna's capability to operate in dual bands and its exceptional performance have been confirmed through rigorous simulation and experimental validation. These results substantiate its reliability and suitability for demanding millimeter-wave applications. The compact design and exceptional performance metrics of the proposed antenna underscore its potential for seamless integration into contemporary wireless communication systems, thereby laying the groundwork for continued progress in SIW and metamaterial-based antenna technology.

1. INTRODUCTION

In the fast-evolving and highly dynamic realm of wireless communication, there is an escalating demand for antennas that can consistently deliver peak performance across a diverse range of frequency bands. Such antennas are essential for modern applications, including fifth-generation (5G) mobile networks, Wi-Fi, and internet of things (IoT) devices. Traditional antenna designs, however, often face challenges in achieving dual-band operation while maintaining a compact form factor and high performance. To address these challenges, this research explores the design and implementation of a SIW cavity-backed dual-band antenna enhanced with metamaterials.

SIW technology has undoubtedly emerged as an exceptionally promising solution for high-frequency antenna designs, boasting inherent advantages such as minimal loss, high-quality factor, and seamless integration with planar circuits. SIW structures confine electromagnetic waves within a dielectric substrate using rows of metallic vias, effectively emulating traditional waveguide behavior. This innovative approach not only effectively reduces the physical dimensions of the antenna but also substantially improves its overall performance, thereby rendering SIW-based antennas exceptionally well suited for a diverse range of advanced communication systems [1].

Metamaterials, on the other hand, have captured substantial attention due to their exceptional electromagnetic properties, which exhibit characteristics not present in natural materials. By engineering the structure at a subwavelength scale, metamaterials can exhibit negative permittivity, permeability, or both, leading to novel electromagnetic phenomena such as negative refraction and electromagnetic bandgaps. These properties can be harnessed to improve antenna performance, such as achieving miniaturization, enhancing bandwidth, and providing multi-band operation [2–4].

Detailed descriptions of miniaturized SIW slot antennas that capitalize on negative order resonance for enhanced performance are presented in [5] and [6]. Metamaterial loading in SIW cavity backed slot antenna (CBSA) enables significant miniaturization to be achieved. A novel design approach for a compact SIW CBSA is outlined in [7]. This design has delivered a gain of 5.4 dBi, an impressive front-to-back ratio (FTBR) of 16.1 dB, and an arrow bandwidth of 1.7% at a frequency of 10 GHz. This paper demonstrates that the impedance bandwidth is influenced by both the substrate thickness and slot width. Furthermore, in [8], a method for enhancing the bandwidth of low-profile CBSA is introduced. The utilization of two hybrid modes has enabled the achievement of a wide bandwidth, leading to an enhanced impedance bandwidth from 1.4% to 6.3%. This was accompanied by a slight improvement in gain.

In [9], the document provides a detailed account of the design and creation of a high-gain, wide bandwidth SIW fed patch antenna array. This array is housed in a multilayer structure that has been specifically engineered for optimal performance within the 60 GHz band. This pioneering antenna design is poised to be a key enabler for upcoming mm-wave wireless communication networks. In the context of satellite communication applications, the presence of a dual-band antenna with a narrow frequency ratio is crucial for accommodating the diverse frequency requirements and ensuring efficient communication across multiple frequency bands. Ref. [10] presents an innovative dual-frequency aperture antenna array tailored

* Corresponding author: Astha Sharma (asthasharma260@gmail.com).

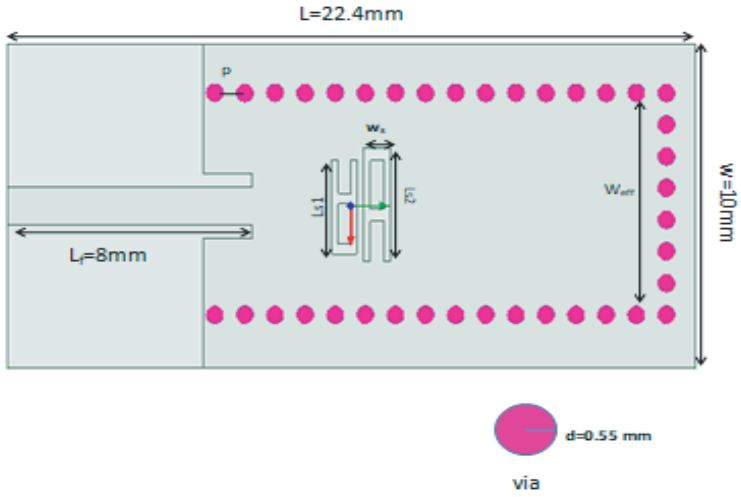

FIGURE 1. SIW structure with two A slots.

for millimeter wave (MMW) bands, specifically the K- and Ka-bands, to address the communication requirements of low earth orbit (LEO) satellites. Ref. [11] provides a comprehensive analysis of the design and demonstration of a compact dual-band CBSA, offering detailed insights into its construction and performance. Additionally, [12] outlines the introduction of a dual-band circularly polarized SIW CBSA. A dual-band SIW CBSA, enhanced with complementary split ring resonator (CSRR) metamaterial, is presented in [13]. This configuration is specifically tailored for applications within the WiMAX/WLAN bands. The antenna is meticulously crafted with a precisely engineered rectangular cavity and strategically positioned CSRR slots on the ground plane, enabling the emission of radiation in two distinct frequency bands. Extensive efforts and substantial research have been dedicated to making advancements in this specific field.

In the context of current work, a novel design has been presented for a dual-band antenna, utilizing a SIW slot array cavity-backed structure. This innovative approach aims to address specific requirements for dual-band communication systems, delivering unparalleled advancements in return loss, efficiency, and radiation characteristics. Moreover, this design offers plethora of advantages including light weight, compact design, excellent performance, and enhanced directivity. Additionally, the design incorporates metamaterial elements to achieve enhanced gain at 27.42 GHz and 28.70 GHz resonance frequencies, thus extending their applications to a diverse range of millimeter wave systems.

2. PROPOSED ANTENNA DESIGN

2.1. SIW Antenna Design with 2 Slots

The intention is to design a cavity-backed SIW antenna for operation in the Ka band, specifically at a frequency of 27 GHz. The antenna's size is carefully selected to ensure optimal performance within this frequency range. The design of the proposed antenna is illustrated in Fig. 1, in detail. It features an inset fed rectangular patch antenna, situated between two intricately designed A-shaped slots within the ground plane. Moreover, the design incorporates a substrate integrated waveguide (SIW) cavity, carefully crafted using a solitary line of metal cylindrical vias encircling the rectangular patch and positioned within the planar substrate. This arrangement effectively forms three of the cavity's side walls, showcasing a sophisticated and innovative approach to antenna engineering. The metallic vias play a crucial role for connecting the radiating patch and ground plane. This interconnection is essential for the effective and coordinated functioning of the antenna system, ensuring the smooth and efficient transmission and reception of signals [14]. The antenna is carefully made on a Rogers RT/Duroid 5880 substrate, which has a permittivity (ε_r) of 2.2, a thickness (h) of 0.508 mm, and an exceptionally low loss tangent ($\tan\delta$) of 0.0009. These specific substrate characteristics are instrumental in ensuring minimal signal loss and optimal performance of the antenna system. The substrate is enhanced with a complex array of closely and uniformly spaced cylindrical metallic vias. These meticulously engineered vias are precisely metalized from the inside, forming a seamless and low-resistance link between the rectangular patch and ground plane, thereby ensuring optimal performance and signal integrity. The propagation of electromagnetic waves within the SIW cavity closely mimics the behavior found within an engineered periodic waveguide due to their similar characteristics and interaction with the surrounding materials. This behavior significantly reduces leakage losses to levels that meet the required standards. Positioning the vias in a manner that obstructs the smooth flow of currents can result in the generation of a significant amount of electromagnetic radiation, potentially impacting the overall performance of the system. Conversely, when the vias are oriented in the path of the current, there will be minimal or no radiation emitted. The existence of spaces between the vias prevents the TM modes from being sustained within the SIW [15]. The proposed antenna has precise physical dimensions of $22.4 \times 10\,\text{mm}^2$, with detailed specifications available

TABLE 1. Antenna dimensions.

L	22.4 mm
W	10 mm
d	0.55 mm
p	0.98 mm
W_f	1.2 mm
L_f	8 mm
L_{s1}	2.9 mm
L_{s2}	3.5 mm
W_s	0.9 mm
w_1	1.8 mm
w_2	1 mm

in Table 1. The proposed antenna design process involved the utilization of Ansys HFSS 2023 software.

The primary objective behind the use of metalized vias is to form the SIW cavity to mitigate the impact of surface wave diffraction at the substrate edges. Additionally, the metalized vias are instrumental in confining the energy below the radiating patch, thereby enhancing the system's comprehensive performance. In this manner, the inclusion of the array of metalized vias contributes to an improvement in the radiation performance, leading to enhanced levels of gain and directivity. To minimize leakage loss, it is important to use vias with a relatively large diameter and position them as closely together as possible. This strategic arrangement helps to effectively contain energy and optimize the performance of the system. The specific dimensions of the proposed antenna directly affect the resonance frequency for the TE_{01} mode of the SIW cavity created by the vias. This correlation is mathematically expressed by the subsequent equation [16, 17]:

$$f_c\left(TE_{10}\right) = \frac{c}{2W_{eff}\sqrt{\varepsilon_r}} \tag{1}$$

$$W_{eff} = W - \frac{d^2}{0.95p} \tag{2}$$

where c represents the velocity of light in vacuum, and ε_r stands for the relative permittivity of the substrate. To effectively reduce the radiation loss between via holes, it is imperative to meticulously determine the dimensions of these vias. By carefully selecting the diameter, spacing, and depth of the via holes, it is possible to significantly minimize electromagnetic radiation and enhance signal integrity in high-frequency circuits. In the context of SIW design, the effective width of the structure, denoted as W_{eff}, plays a pivotal role. This width is determined by the dimensions of the vias within the structure. Specifically, the parameter 'd' corresponds to the vias diameter, while 'p' denotes the inter-via spacing. Additionally, in this context, 'W' represents the rectangular waveguide width. The objective is to carefully select these dimensions to minimize radiation loss in order to ensure that

$$\frac{p}{\lambda_c} < 0.25 \tag{3}$$

$$d < \lambda_g/5 \tag{4}$$

$$d < p < 2d \tag{5}$$

where λ_c and λ_g are the cut-off wavelength and guided wavelength, respectively. First, the investigation of the structure's parameters is carried out by applying only two slots on the top of the SIW cavity. The gap between the slots is taken to be 0.224 mm. The initial selection pertaining to the slots is made in close proximity to the distance between the via walls, and they are subsequently optimized to achieve the exact resonant frequency. Subsequently, the optimization process entails adjusting the slot widths to achieve the desired performance parameters. Furthermore, the simulated S-parameters display highly favorable return loss characteristics at a specific resonant frequency of 27.50 GHz, as clearly shown in Fig. 2. This indicates the strong performance of the system at a precise frequency point. Additionally, the design demonstrates an impressive 10 dB return loss bandwidth spanning approximately 550 MHz. Further, Fig. 3 illustrates the surface current distribution of the antenna design featuring two slots. Notably, the resonant frequency yields a substantial gain of 5.72 dBi, as visually indicated in Fig. 4.

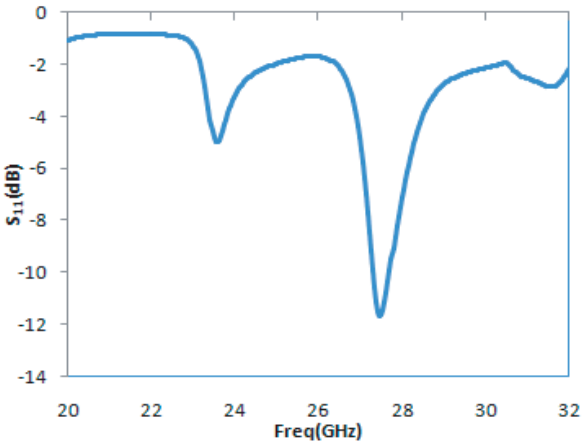

FIGURE 2. S parameter graph for SIW structure with two A slots.

2.2. SIW Antenna Design with 4 Slots

The characteristics of the structure with four slots as radiating elements depicted in Fig. 5(a) are analyzed in this section. The inclusion of four slots enables enhanced control over the configuration of the operating frequency ranges of the cavity-backed antenna. A comparison is made between the effectiveness of cavity-backed antennas with two slots and those with four slots to assess the enhanced behavior of the structure. The graph in Fig. 5(b) illustrates the simulated return loss of the proposed design. The evaluation of the proposed configuration indicates that by incorporating slots, the structure exhibits resonance at two distinct frequencies of 27.42 GHz and 28.70 GHz. Furthermore, it demonstrates an impedance bandwidth (-10 dB) of 380 MHz and 300 MHz at the first and second resonance frequencies, respectively. It is also noticed from the simulated graph of reflection coefficient that increase in the number of slots enhances the return loss value as compared to that of two slots. The simulated gains of the antenna are depicted in Fig. 7

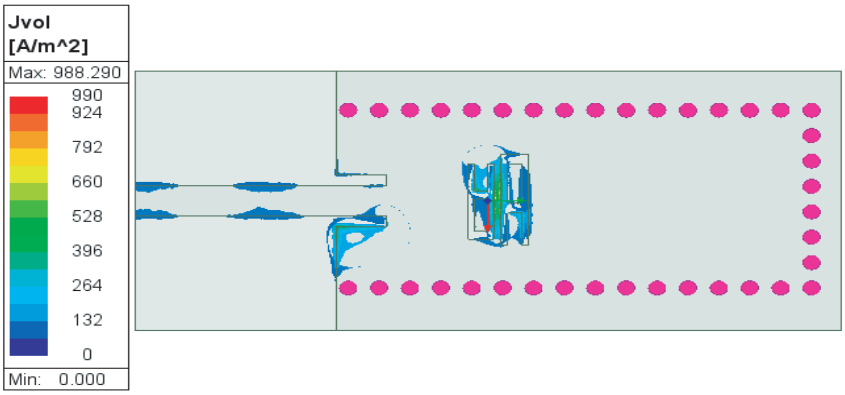

FIGURE 3. Surface current plot of SIW structure with two A slots.

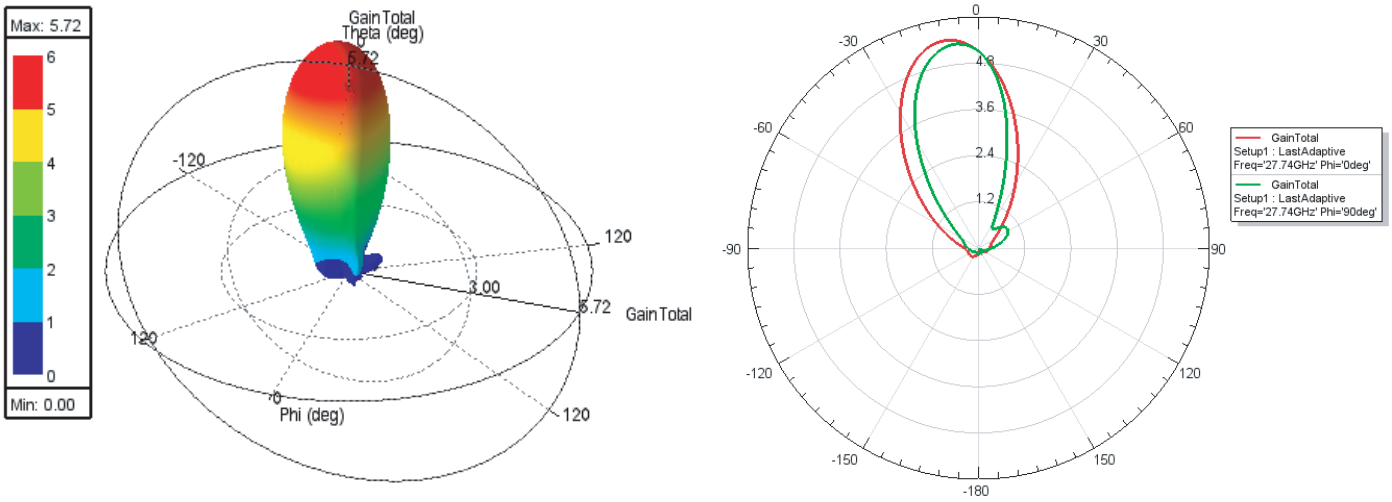

FIGURE 4. Three-dimensional and two-dimensional gain representations of SIW structure with two slots.

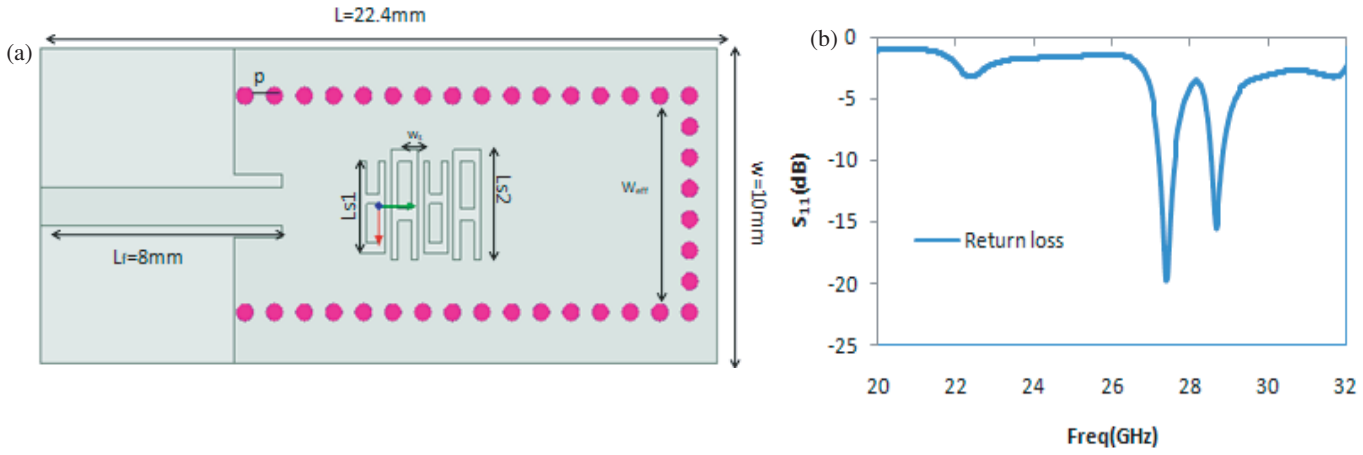

FIGURE 5. (a) SIW structure with four A slots. (b) Reflection Coefficient of SIW structure with four A slots.

and Fig. 8 at two resonant frequencies which are respectively 6.29 dBi and 4.64 dBi. 2-D and 3-D representations of radiation pattern are also shown in Fig. 7 and Fig. 8, which show pencil beam having maximum lobes known as 2D and 3D polar plots. The simulation results have provided a SIW antenna with negligible back lobes and minimum side lobes, and highly directive beam is formed with maximum radiation at both the resonant frequencies. The achieved directive radiation pattern makes

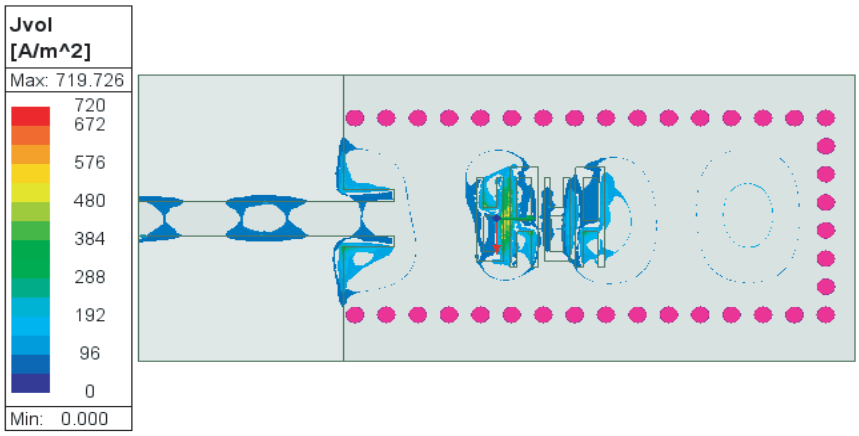

FIGURE 6. Surface current distribution of SIW structure with four A slots.

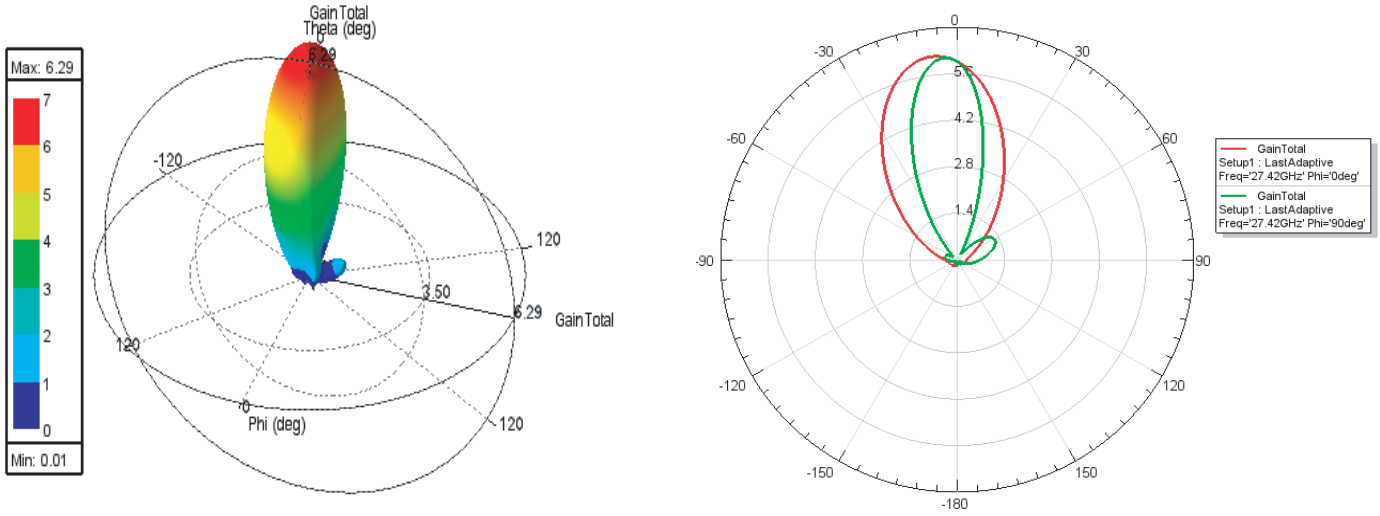

FIGURE 7. Three-dimensional and two-dimensional gain representations of SIW structure with four A slots at 27.42 GHz.

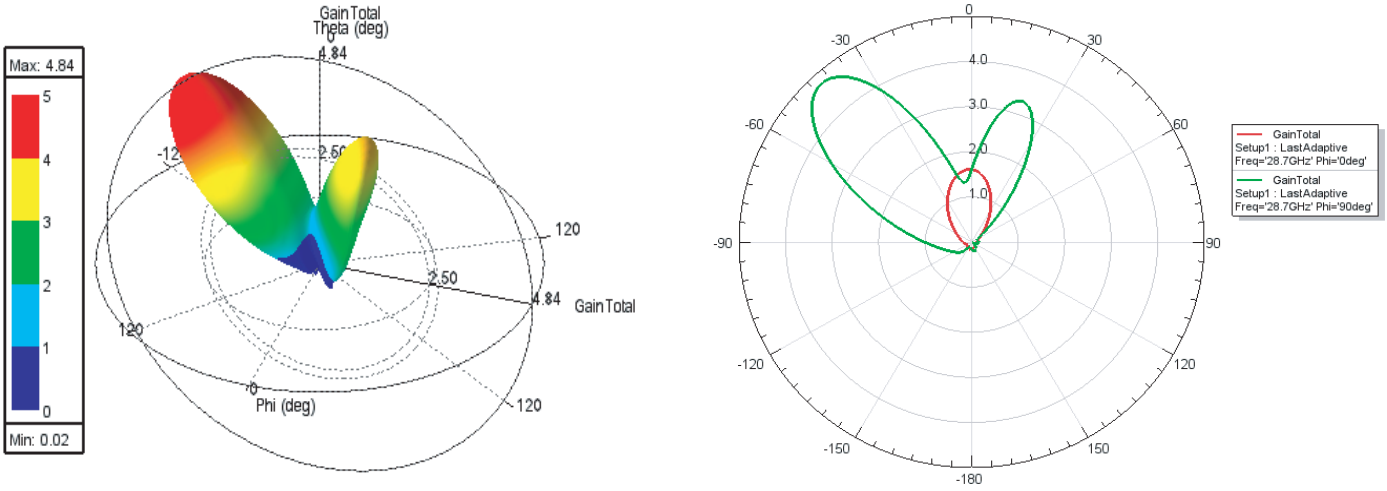

FIGURE 8. Three-dimensional and two-dimensional gain representations for SIW antenna structure with four A slots at 28.70 GHz.

TABLE 2. Comparison of the performance between the designed and previously reported work.

Ref.	RF (GHz)	IBW (MHz)	Gain (dBi)	RL (dB)	Size (mm^2)	MTM	RE	WS
[13]	2.5/5.4	100/130	3.43 dBi and 5.31 dBi	$> 17/ > 25$	30×30	CSRR	NR	WLAN
[24]	9.5/13.85	173/200	4.8 dBi and 3.74 dBi	$> 20/ > 15$	24×20	No	NR	X band, K_U band
[25]	9.5/10.5	520/450	6.66 dBi and 6.44 dBi at	$> 10/ > 20$	17×16	No	NR	X band,
[26]	4.9/5.93	400/200	3.7 dBi and 1.4 dBi	$> 20/ > 20.$	60×60	No	NR	U-NII-1 band
[27]	2.23/2.98/3.42 /4.82/5.71 /11.61/12.51	280/130/150 /330/190 /500/1000	1.94/2.2/1.66 /3.87/3.65 /4.06/4.14	$> 15/ > 25$ $/ > 15 > 15$ $/ > 20/ > 10$ $/ > 20$	35×34	SRR, CSRR	41.5/48.6 /58.1/60.1 /84.4/78.7 /82.1	WLAN, WiMAX, RFID, Upper X band, Lower K_U band
[28]	3.3/5.0 /5.8/6.6/ 9.9/15.9	140/560 /440/540 /410/900	2.72/3.81 /2.12/2.78 /3.68/4.10	$> 15/ > 30$ $/ > 30/ > 15$ $/ > 35 > 20$	44×39	SRR	41.2, 84.7, 52.8, 69.7 78.8, 76.9	upper WLAN, lower WiMAX, super extended C-band, middle X band, lower K_U band
[29]	2.42/4.34 /5.81/8.45 /11.02/13.98 16.12/18.87	480,/640 /370/900 /2.38 GHz /660/1.68 GHz /1.65 GHz	2.31/2.67 /2.98/2.49 /3.84/2.29 /3.61/4.23	$> 35/ > 15$ $/ > 25/ > 15$ $/ > 15 > 10$ $> 20 > 30$	32×22	SRR, CSRR	68.24/62.43 /79.84/78.91 /81.02/61.12 /78.84/81.78	S, C, X, Ku, K
This Work	27.42/28.30	380/300	6.40/4.77	$> 17.5/ > 15$	22.4×10	SRR	95.2/95.7	Ka-band

Ref—Reference, RF—Radio Frequency, IBW—Impedancel Bandwidth, IL—Insertion Loss, RL—Return Loss, NR—Not Reported, NA—Not applicable, RE—Radiation Efficiency, WS—Wireless Standards.

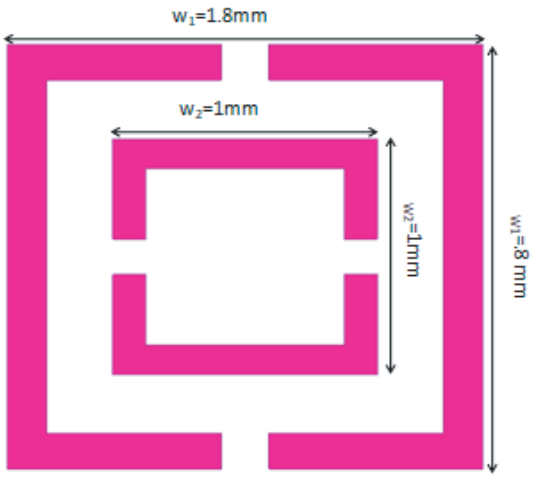

FIGURE 9. Metamaterial Unit cell.

this antenna well suited for focussed communication systems operating specifically in mm-wave frequency bands [18]. The surface current distribution, as depicted in Fig. 6, reveals a notable flow of current into the slots through the pair of connecting strips.

2.3. SIW Antenna Design with SRR Metamaterial

Metamaterials are artificial electromagnetic materials with novel effective medium properties that may not be available in nature. These materials are created by arranging components at the subwavelength scale, allowing them to manipulate electromagnetic waves in unique ways. It is possible to obtain negative values for permittivity and permeability by using proper designs of metamaterials. The development and implementation of metamaterial structures have significantly expanded the possibilities for designing innovative circuits and enhancing the performance of individual components. These advancements open up a prospective array of

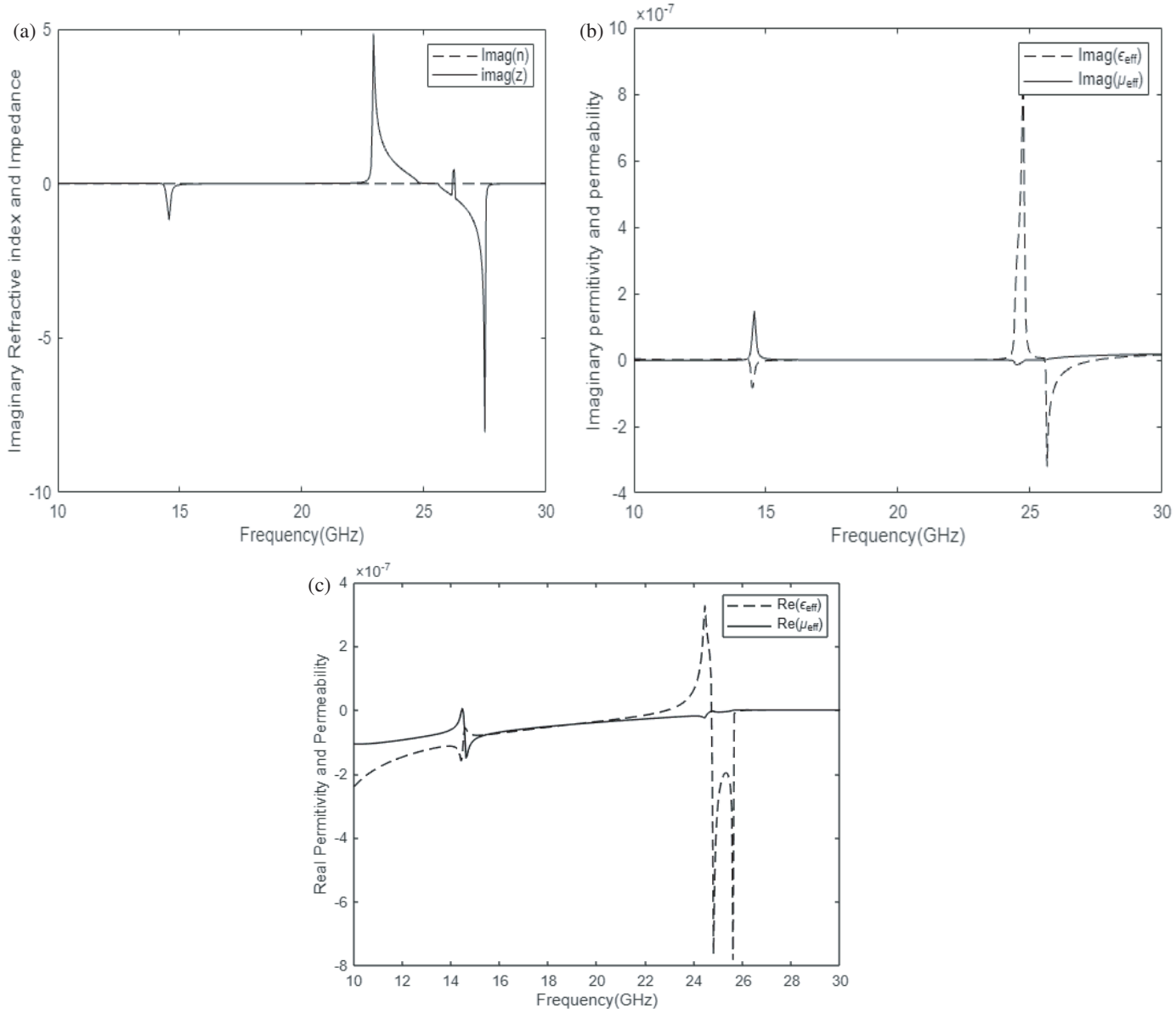

FIGURE 10. (a) Refractive index and impedance of MTM. (b) Imaginary Permittivity and permeability of MTM. (c) Real Permittivity and permeability of MTM.

applications across various fields, including satellite communications [19–23]. In this section, an SRR metamaterial (MTM) is meticulously designed and implemented on a 0.508 mm thick base composed of Rogers RT/duroid 5880. This substrate has a specific dielectric constant of 2.2 and a low loss tangent of 0.0009. The detailed configuration is illustrated in Fig. 9. To enhance the gain characteristics, a split ring loaded with metamaterial is strategically introduced in close proximity to the feed line. By employing periodic boundary conditions, the effective parameters of the MTM are derived, as depicted in the illustration. The MTM unit cell's outer ring has a size of 1.8 mm, while the inner ring has a measurement of 1 mm.

The Smith method and MATLAB software are employed to precisely calculate the effective values of dielectric constant, magnetic permeability, and index of refraction for the metamaterial element, utilizing the simulated S-parameters. With respect to frequency, Fig. 10(a) presents the variation of the unit cell refractive index, while Figs. 10(b) and 10(c) illustrate the imaginary and real parts of the effective dielectric constant and magnetic permeability. Furthermore, due to the exceptionally low effective permeability, the metamaterial exhibits a very low effective normalized intrinsic impedance in the vicinity of that frequency. The plot in Fig. 10(b) illustrates that the imaginary components of the relative effective electric permittivity and magnetic permeability are close to zero. This suggests that the MTM structure exhibits minimal loss. In addition, the data presented in Fig. 10(c) reveal that for frequencies above 25 GHz, the relative effective electric permittivity and magnetic permeability both exhibit negative values, thus providing strong evidence supporting the metamaterial behavior of the consid-

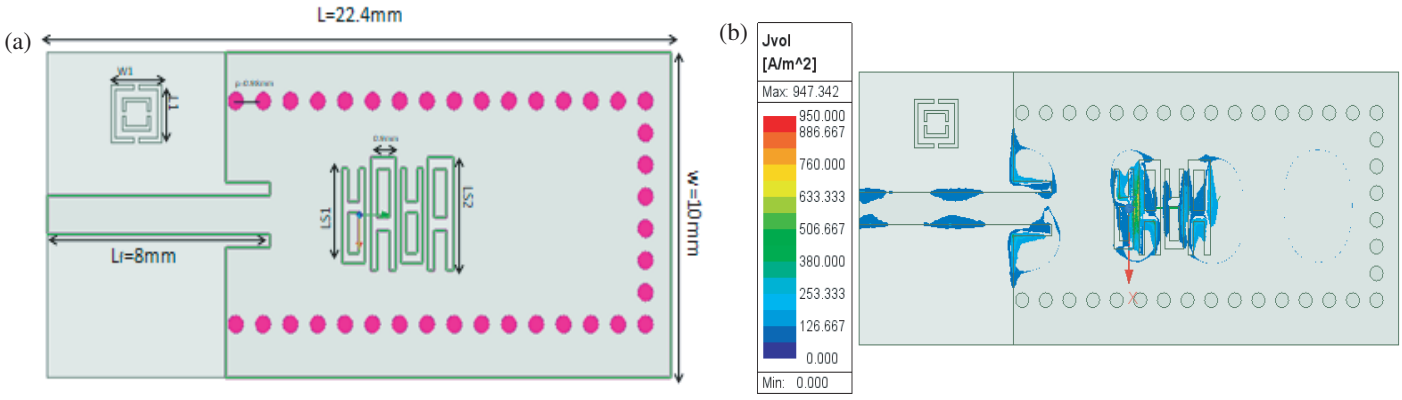

FIGURE 11. (a) SIW structure with 4 slots and a single MTM. (b) Surface current distribution.

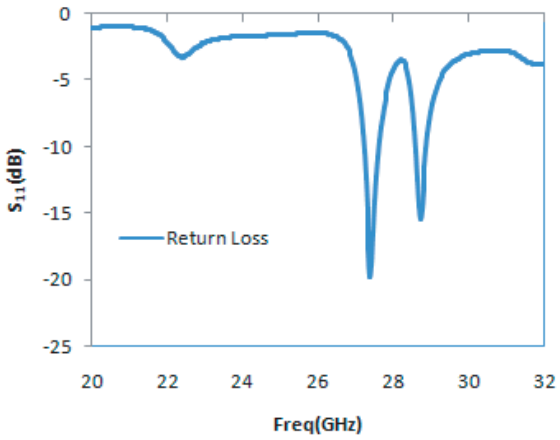

FIGURE 12. S parameter graph of SIW structure with four A slots and single MTM.

ered MTM element. The low-impedance characteristics of this MTM within the 25–30 GHz frequency range are leveraged in the upcoming section to boost the gain of a SIW cavity-backed antenna.

A single metamaterial unit cell in design has been added as shown in Fig. 11(a) which depicts the surface current distribution as shown in Fig. 11(b). The figure depicting the S_{11} (dB) of the SIW cavity backed antenna with the integrated metamaterial is displayed in Fig. 12. As can be observed from Fig. 13 and Fig. 14, it is evident that the antenna equipped with a single MTM achieves a gain of 6.34 dBi at the resonant frequency of 27.42 GHz and a gain of 4.74 dBi at 28.70 GHz, respectively. Upon the addition of two MTMs as shown in Fig. 15, the antenna demonstrates gains of 6.40 dBi and 4.77 dBi at two resonant frequencies, as shown in Figs. 18 and 19, respectively. Fig. 16 clearly presents the S parameter plot for the structure incorporating two metamaterial unit cells. Furthermore, the surface current distributions are effectively shown in Fig. 17 at frequencies of 27.42 GHz and 28.70 GHz, respectively. Therefore, upon careful observation, it becomes apparent that there is a slight boost in the gain with the addition of metamaterial at both resonant frequencies compared to the proposed design without MTM.

A comprehensive parametric analysis is conducted to analyze the impact of various positions of the slot and MTM unit cell on the overall system behavior. It is apparent from the simulated response that altering the position of the slot causes a shift in the return loss value at both resonant frequencies as shown in Fig. 20. As the position of the slot is varied from 0.2 mm to 1.2 mm, a corresponding increase in the return loss value is observed, indicating a potential decline in impedance matching. Additionally, there is a slight shift in the lower resonating frequency. This behavior highlights the significance of precise slot positioning in achieving the desired operational characteristics of the system. However, despite changes in the position of the slot, no shift in the upper resonating frequency has been observed. In contrast, there is an increase in the return loss value, which may indicate a deterioration in impedance matching and a decrease in energy transmission efficiency in this frequency range. Furthermore, as the position of the metamaterial (MTM) element is adjusted between -0.4 mm and 0.4 mm, it has been observed that there is no discernible shift in either the lower or upper resonating frequency. However, a slight increase in the return loss value of the designed antenna is noted at both frequencies. This indicates a decrease in impedance matching, suggesting that the adjustment of the MTM element's position affects the antenna's efficiency in energy transmission, even though the resonating frequencies remain stable. This observation emphasizes the importance of positioning the MTM element to optimize antenna performance.

3. EXPERIMENTAL VALIDATION

The antenna under consideration is constructed using a printed circuit board (PCB) prototyping machine. The illustration depicting the fabricated antenna, along with the testing setup within an anechoic chamber, is presented in Fig. 21. The S_{11} (dB) of the fabricated antenna is assessed utilizing the Anritsu Vector Network Analyzer, which provided valuable insights into its performance. The experimental and simulated S_{11} (dB) responses of the designed antenna are illustrated in Fig. 22. Fig. 23 depicts the gain representation specifically over

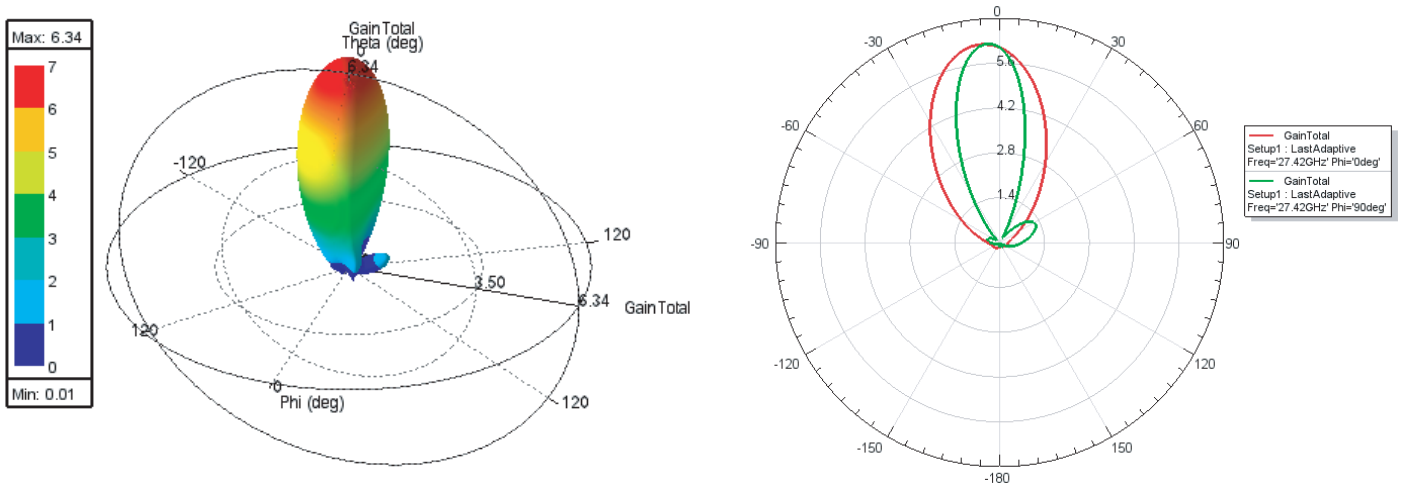

FIGURE 13. Three-dimensional and two-dimensional gain representations of SIW antenna structure with slot array and a single MTM at 27.42 GHz.

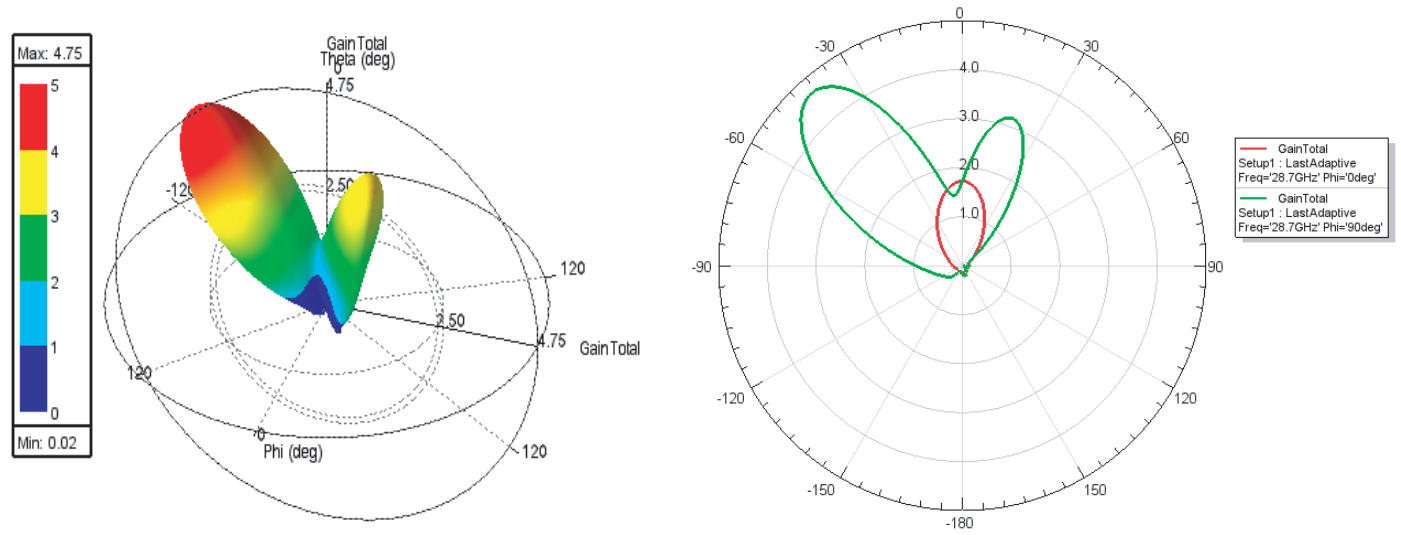

FIGURE 14. Three-dimensional and two-dimensional gain representations of SIW antenna structure with slot array and single MTM at 28.70 GHz.

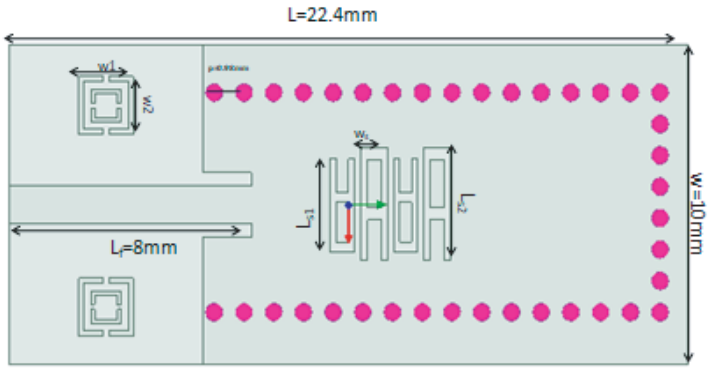

FIGURE 15. SIW antenna structure with slot array and two metamaterial.

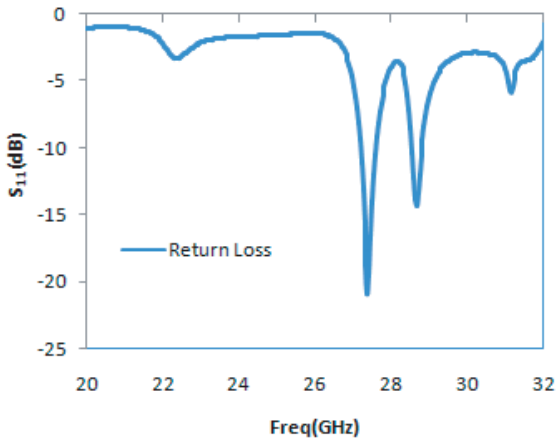

FIGURE 16. S parameter plot of SIW antenna structure with slot array and two metamaterial.

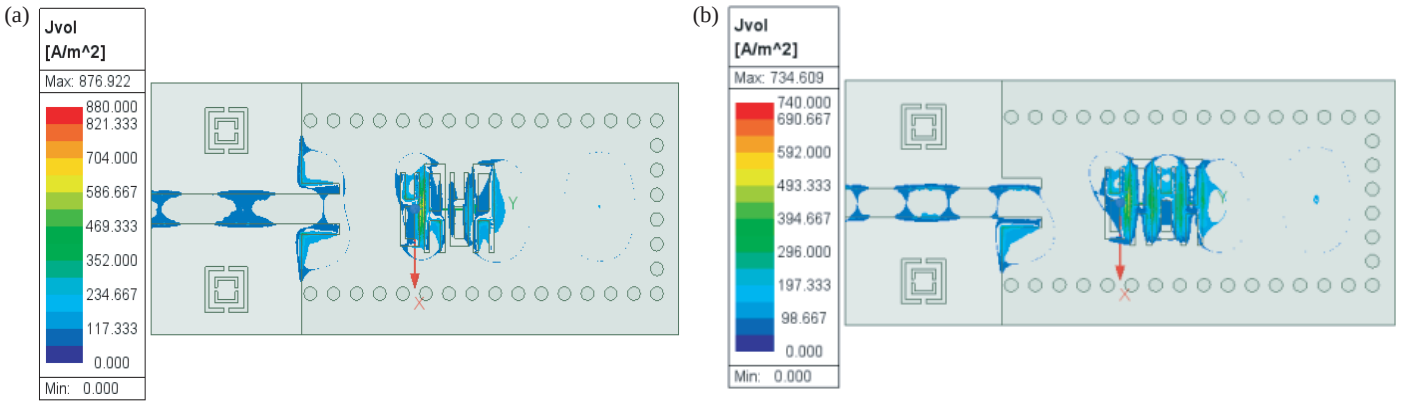

FIGURE 17. Surface current of SIW antenna structure with slot array and two metamaterials at (a) 27.42 GHz and (b) 28.70 GHz.

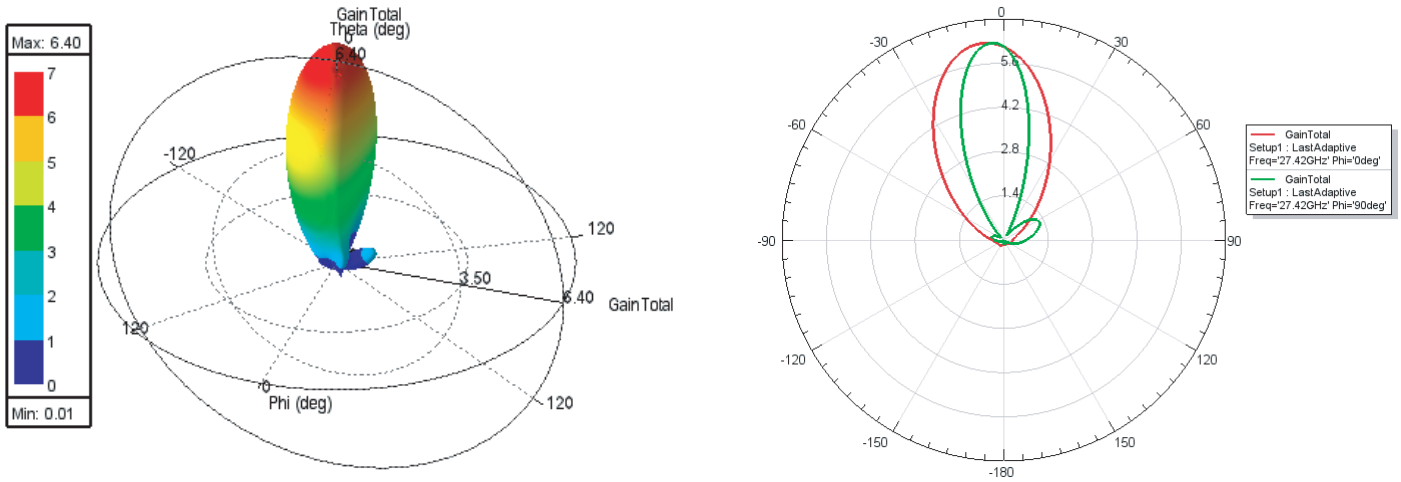

FIGURE 18. Three-dimensional and two-dimensional gain representations of SIW antenna structure with slot array and two metamaterials at 27.42 GHz.

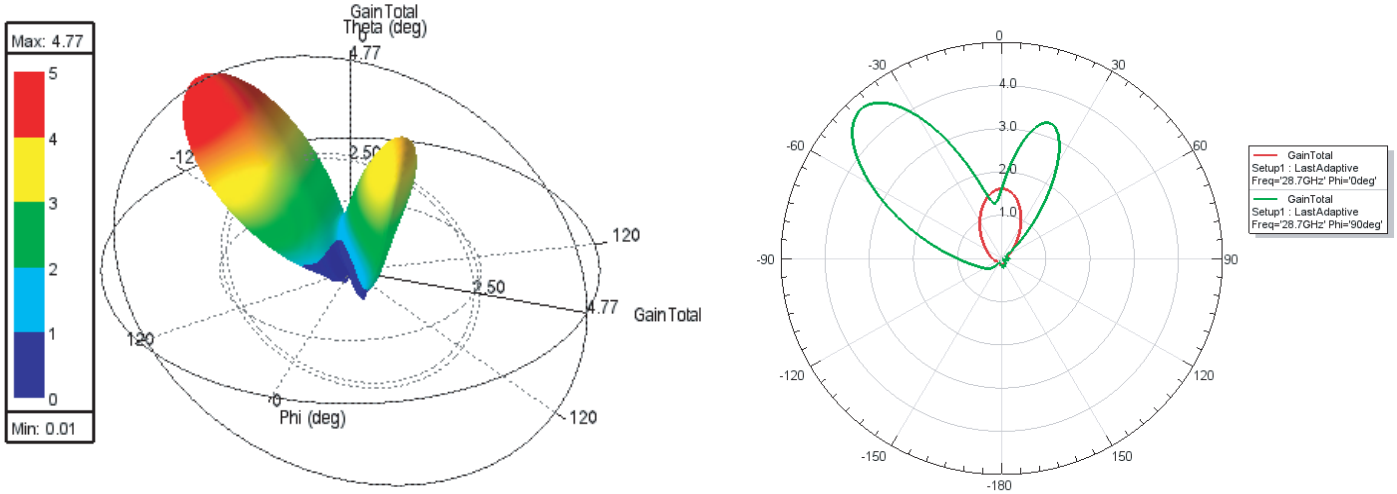

FIGURE 19. Three-dimensional and two-dimensional gain representations of SIW antenna structure with slot array and two metamaterials at 28.70 GHz.

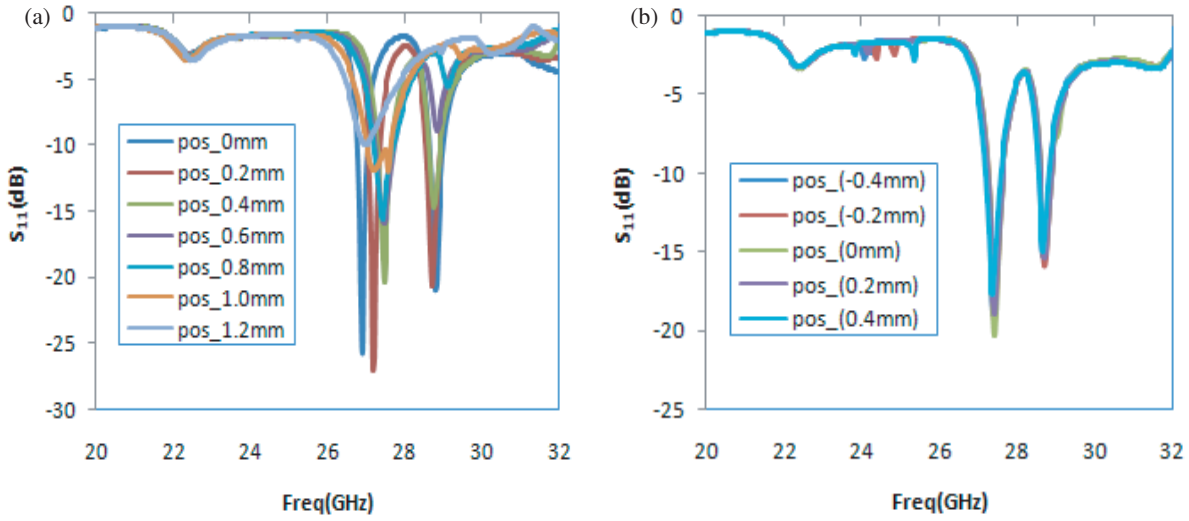

FIGURE 20. Parametric analysis on position of (a) A slot, (b) MTM unit cell.

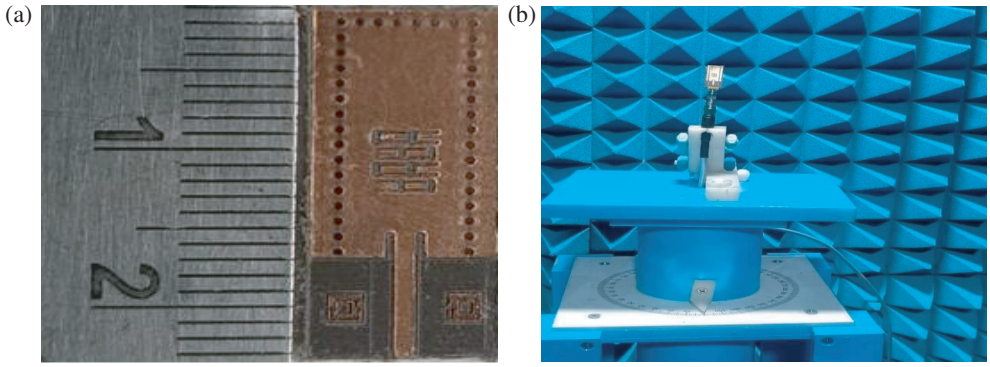

FIGURE 21. Photograph of the proposed antenna. (a) Fabricated prototype. (b) Anechoic chamber setup for measurement .

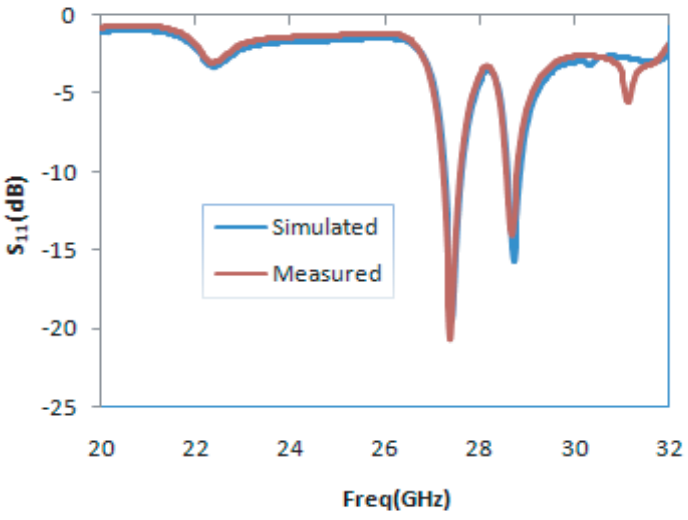

FIGURE 22. S parameter graph of SIW structure with four A slots and two MTMs.

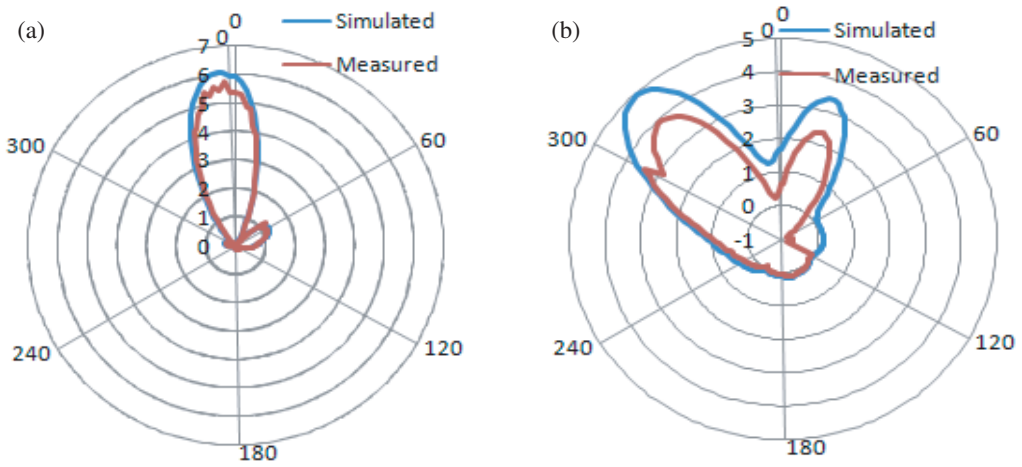

FIGURE 23. Gain representation. (a) 27.42 GHz. (b) 28.7 GHz.

the dual-band radiation at 27.42 GHz and 28.70 GHz. In Table 2, a performance comparison between the designed dual frequency antenna and relevant previously reported research studies is provided.

4. CONCLUSION

The innovative antenna design showcases a compact structure, utilizing an SRR loaded SIW slot array cavity. This configuration enables the antenna to emit radiation across two distinct frequency bands, making it a versatile solution for wide range of applications. By increasing the number of slots, it has been observed that the antenna is capable of achieving dual bands. This phenomenon demonstrates the relationship between the slot configuration and the antenna's dual band performance. Furthermore, the investigation highlights the significance of integrating an SRR along with the rectangular SIW cavity resonator to improve the antenna's gain. Parametric analysis has been used to thoroughly explain the effectiveness of the proposed configuration. The antenna that is fabricated possesses a compact design, and its radiation properties have been meticulously scrutinized through testing and analysis to provide detailed insights into its performance. The measured radiation pattern exhibits distinctive unidirectional power levels, specifically tailored to meet the requirements of 27.42 GHz and 28.70 GHz satellite applications. This indicates a specialized and precise performance designed to cater to the characteristics of these specific frequencies.

REFERENCES

[1] Aparna, E., G. Ram, and G. A. Kumar, "Review on substrate integrated waveguide cavity backed slot antennas," *IEEE Access*, Vol. 10, 133 504–133 525, 2022.

[2] Murad, N. A., M. W. Almeshehe, O. Ayop, and M. K. A. Rahim, "Wideband metamaterial substrate integrated waveguide antenna for millimeterwave applications," in *2020 IEEE International RF and Microwave Conference (RFM)*, 1–4, Kuala Lumpur, Malaysia, Dec. 2020.

[3] Krushna Kanth, V. and S. Raghavan, "EM design and analysis of a substrate integrated waveguide based on a frequency-selective surface for millimeter wave radar application," *Journal of Computational Electronics*, Vol. 18, 189–196, 2019.

[4] Cai, Y., Y. Zhang, L. Yang, Y. Cao, and Z. Qian, "Design of low-profile metamaterial-loaded substrate integrated waveguide horn antenna and its array applications," *IEEE Transactions on Antennas and Propagation*, Vol. 65, No. 7, 3732–3737, Jul. 2017.

[5] Dong, Y. and T. Itoh, "Miniaturized substrate integrated waveguide slot antennas based on negative order resonance," *IEEE Transactions on Antennas and Propagation*, Vol. 58, No. 12, 3856–3864, Dec. 2010.

[6] Saghati, A. P., A. P. Saghati, and K. Entesari, "An ultra-miniature SIW cavity-backed slot antenna," *IEEE Antennas and Wireless Propagation Letters*, Vol. 16, 313–316, 2016.

[7] Luo, G. Q., Z. F. Hu, L. X. Dong, and L. L. Sun, "Planar slot antenna backed by substrate integrated waveguide cavity," *IEEE Antennas and Wireless Propagation Letters*, Vol. 7, 236–239, 2008.

[8] Luo, G. Q., Z. F. Hu, W. J. Li, X. H. Zhang, L. L. Sun, and J. F. Zheng, "Bandwidth-enhanced low-profile cavity-backed slot antenna by using hybrid SIW cavity modes," *IEEE Transactions on Antennas and Propagation*, Vol. 60, No. 4, 1698–1704, Apr. 2012.

[9] Li, Y. and K.-M. Luk, "Low-cost high-gain and broadband substrate-integrated-waveguide-fed patch antenna array for 60-GHz band," *IEEE Transactions on Antennas and Propagation*, Vol. 62, No. 11, 5531–5538, Nov. 2014.

[10] Guo, Z.-J., Z.-C. Hao, H.-Y. Yin, D.-M. Sun, and G. Q. Luo, "Planar shared-aperture array antenna with a high isolation for millimeter-wave low earth orbit satellite communication system," *IEEE Transactions on Antennas and Propagation*, Vol. 69, No. 11, 7582–7592, Nov. 2021.

[11] Li, W., K. D. Xu, X. Tang, Y. Yang, Y. Liu, and Q. H. Liu, "Substrate integrated waveguide cavity-backed slot array antenna using high-order radiation modes for dual-band applications in K-band," *IEEE Transactions on Antennas and Propagation*, Vol. 65, No. 9, 4556–4565, Sep. 2017.

[12] Wu, Q., J. Yin, C. Yu, H. Wang, and W. Hong, "Low-profile millimeter-wave SIW cavity-backed dual-band circularly polarized antenna," *IEEE Transactions on Antennas and Propagation*, Vol. 65, No. 12, 7310–7315, Dec. 2017.

[13] Daniel, R. S., "Dual-band SIW cavity backed antenna loaded with CSRR metameterial," *Microsystem Technologies*, Vol. 29, No. 3, 337–345, 2023.

[14] Kumar, A., M. Kumar, and A. K. Singh, "Substrate integrated waveguide cavity backed wideband slot antenna for 5G applications," *Radioengineering*, Vol. 30, No. 3, 480–487, 2021.

[15] Xu, F. and K. Wu, "Guided-wave and leakage characteristics of substrate integrated waveguide," *IEEE Transactions on Microwave Theory and Techniques*, Vol. 53, No. 1, 66–73, 2005.

[16] Deslandes, D. and K. Wu, "Integrated microstrip and rectangular waveguide in planar form," *IEEE Microwave and Wireless Components Letters*, Vol. 11, No. 2, 68–70, Feb. 2001.

[17] Deslandes, D. and K. Wu, "Integrated transition of coplanar to rectangular waveguides," in *2001 IEEE MTT-S International Microwave Sympsoium Digest (Cat. No.01CH37157)*, Vol. 2, 619–622, May 2001.

[18] Job, M., R. S. Yadav, M. G. Siddiqui, V. Gahlaut, and U. N. Mishra, "High-gain pencil-beam microstrip antenna array for radar application," *Progress In Electromagnetics Research Letters*, Vol. 113, 17–24, 2023.

[19] Bhowmik, W., B. Appasani, A. K. Jha, and S. Srivastava, "A review on metamaterial application in microstrip and substrate integrated waveguide antenna designs," *Progress In Electromagnetics Research B*, Vol. 96, 87–132, 2022.

[20] Alu, A., N. Engheta, A. Erentok, and R. W. Ziolkowski, "Single-negative, double-negative, and low-index metamaterials and their electromagnetic applications," *IEEE Antennas and Propagation Magazine*, Vol. 49, No. 1, 23–36, 2007.

[21] Milias, C., R. B. Andersen, P. I. Lazaridis, Z. D. Zaharis, B. Muhammad, J. T. B. Kristensen, A. Mihovska, and D. D. S. Hermansen, "Metamaterial-inspired antennas: A review of the state of the art and future design challenges," *IEEE Access*, Vol. 9, 89 846–89 865, 2021.

[22] Jokanović, B., R. H. Geschke, T. S. Beukman, and V. Milošević, "Metamaterials: Characteristics, design and microwave applications," *SAIEE Africa Research Journal*, Vol. 101, No. 3, 82–92, 2010.

[23] Veselago, V. G., "The electrodynamics of substances with simultaneously negative values of Ɛ and μ," *Soviet Physics Uspekhi*, Vol. 10, 509–514, 1967.

[24] Mukherjee, S., A. Biswas, and K. V. Srivastava, "Substrate integrated waveguide cavity-backed dumbbell-shaped slot antenna for dual-frequency applications," *IEEE Antennas and Wireless Propagation Letters*, Vol. 14, 1314–1317, 2014.

[25] Luo, G. Q., Z. F. Hu, Y. Liang, L. Y. Yu, and L. L. Sun, "Development of low profile cavity backed crossed slot antennas for planar integration," *IEEE Transactions on Antennas and Propagation*, Vol. 57, No. 10, 2972–2979, Oct. 2009.

[26] Sengupta, R., S. Banerjee, and M. Mitra, "A typical slotted SIW cavity-backed antenna for dual frequency operations in U-NII bands," *Advanced Electromagnetics*, Vol. 12, No. 3, 19–26, May 2023.

[27] Saraswat, R. K. and M. Kumar, "A metamaterial hepta-band antenna for wireless applications with specific absorption rate reduction," *International Journal of RF and Microwave Computer-Aided Engineering*, Vol. 29, No. 10, e21824, 2019.

[28] Saraswat, R. K. and M. Kumar, "A vertex-fed hexa-band frequency reconfigurable antenna for wireless applications," *International Journal of RF and Microwave Computer-Aided Engineering*, Vol. 29, No. 10, e21893, Oct. 2019.

[29] Saraswat, R. K. and M. Kumar, "Implementation of the metamaterial multiband frequency reconfigurable antenna for IoT wireless standards," *IETE Journal of Research*, Vol. 70, No. 5, 4594–4605, 2024.